Effect of Delamination of Axially Loaded Homogeneous Laminated Plates

G. J. Simitses,* S. Sallam,† and W. L. Yin‡
Georgia Institute of Technology, Atlanta, Georgia

A simple one-dimensional model has been developed and analyzed for predicting delamination buckling loads. The model is employed to predict critical loads for delaminated homogeneous plates with both simply supported and clamped ends. The effects of delamination position, size, and thickness on the critical loads are studied in detail for both sets of boundary conditions. The results reveal that for certain geometries the buckling load can serve as a measure of the load carrying capacity of the delaminated configuration. In other cases, the buckling load is very small and delamination growth is a strong possibility, depending on the toughness of the material.

I. Introduction

THE constant demand for lighter and more efficient structural configurations has led the structural engineer to the use of fiber reinforced composites. At the same time, this demand forced upon him very sophisticated methods of testing, of analysis and design, as well as of fabrication and manufacturing. The recent explosive progress in producing and using composite materials has pointed toward the clear possibility of creating specific materials for specific missions. A testimony to this is the present wide use of laminated plates and shells as primary structural components.

In addition to the usual geometric imperfections that are inherent in metallic plates and shells, laminated geometries are prone to such defects as broken fibers, cracks in the matrix materials, and delaminated areas (separation of adjoining plies). Delaminations are developed as a result of imperfections in production technology or the effect of certain factors during the operational life of the laminate, such as impact by foreign objects. Because of this, the delamination can be located in various places relative to the bounding surfaces of the geometry. Regardless of its origin or location, delamination may reduce the load carrying capacity of the laminate and, thus, affect greatly the safety (damage tolerance) of the system.

Problems of delamination growth in composites have received attention in recent years. A fairly extensive review may be found in Ref. 1 and its cited references. More recently, the problem of delamination buckling and growth was dealt with by several investigators. Troshin[2] addressed primarily the question of delamination buckling in dealing with a pressure-loaded laminar cylindrical shell. He assumed that a delamination exists over a small part of the circumference, somewhere between the bounding surfaces of the shell, and that it extends along the entire length of the cylinder. He found critical pressures for various locations and sizes of the delamination. The problem of delamination buckling and growth for a laminated plate was addressed by Chai et al.[3] They presented a one-dimensional model describing the failure mechanism. They also presented analyses for both a thin film delamination model (the delamination divides the thickness into a large and a very small part) and a general model (the two parts are virtually of equal thickness). In both models the emphasis is placed on studying the delamination growth by employing the fracture (toughness) energy of the system. The paper gives primarily a good description of and insight into the phenomenon of delamination growth. There exist only a few more papers that deal with instability-related delaminations growth.[4-7]

This paper deals primarily with the question of delamination buckling (as in Ref. 2) and how the presence of the delamination affects the global load carrying capacity of the laminated plate.

II. Mathematical Formulation

A one-dimensional modeling of the laminated plate is employed similar to the one used in Ref. 3. The inherent assumptions of this modeling include: 1) the properties of the plate are homogeneous and, at most, orthotropic; 2) the material behavior is linearly elastic; and 3) delamination exists and grows (if it does) along a plane parallel to the reference plane. This simplified modeling is employed in order to understand better and give more attention to the physical behavior, rather than get involved (and lost) in a more complex model with several additional parameters and a considerably more difficult solution scheme. In accordance with this philosophy, it is also assumed that the delamination exists before the compressive loading is applied. The location and length (size) of the delamination are arbitrary and the ends of the plate are either hinged or clamped (see Fig. 1). Note that, because of the one-dimensional modeling, the sides of the plate are free. Finally, it is assumed that the delamination separates the column (or plate) into four regions, each having such dimensions (lengths and thicknesses) that Euler-Bernoulli beam theory is applicable (this assumption may also be removed by employing more accurate theories for small length to thickness ratios).

The three axes of orthotropy are parallel to the reference frame x, y, z. The natural plane of the plate lies on the x-z plane. The plate is of unit width and is subjected to a uniform compressive load P along the supported edges. A layer of uniform but arbitrary thickness h and of length a is delaminated (see Fig. 1). The delamination extends across the entire width of the plate (one-dimensional modeling).

Presented as Paper 84-0964 at the AIAA/ASME/ASCE/AHS 25th Structures, Structural Dynamics and Materials Conference, Palm Springs, CA, May 14-16, 1984; received July 20, 1984; revision received Nov. 1, 1984.

*Professor, Engineering Science and Mechanics. Associate Fellow AIAA.
†Graduate Research Assistant, Engineering Science and Mechanics.
‡Associate Professor, Engineering Science and Mechanics.

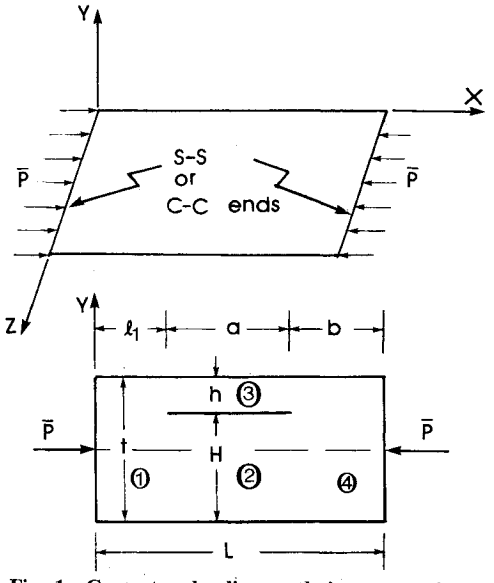

Fig. 1 Geometry, loading, and sign convention.

Note from Fig. 1 that the delamination divides the plate (column) into four regions, 1-4. The coordinate system is such that x is measured from the left end. Moreover, u_i and v_i $(i=1,2,3,4)$ denote the in-plane and transverse displacements of material points on the midplane of each region (each part). For example, v_3 is the transverse displacement of material points on the plane $h/2$ units from the top surface (region 3), while v_2 is the transverse displacement of material points on the plane $H/2$ units from the bottom surface (region 2). Furthermore, note that because of the Euler-Bernoulli assumptions $v_i(x)$ characterizes the transverse displacement of every material point in region i and position x. Similarly, the in-plane displacement, $u_i(x,y_i)$, of every material point is given by

$$\bar{u}_i(x,y_i)=u_i(x)-y_i v_{i,x} \tag{1}$$

where y_i is measured from the midsurface of each region and the comma denotes differentiation with respect to the index that follows. The necessary equations, including kinematic relations, constitutive relations, relations between loads and moments on one side and kinematic parameters on the other, and equilibrium equations, are given as follows.

$$\epsilon_{xx_i}=\epsilon^0_{xx_i}-y_i v_{i,xx} \qquad \epsilon^0_{xx_i}=u_{i,x}+\tfrac{1}{2}v^2_{i,x} \tag{2}$$

$$\sigma_{xx_i}=(E_{xx}\epsilon_{xx_i})\S \tag{3}$$

$$P_i=\int_{A_i}\sigma_{xx_i}\mathrm{d}A_i=E_{xx}A_i\epsilon^0_{xx_i}=C_{xx_i}\epsilon^0_{xx_i}$$

$$M_i=-\int_{A_i}y_i\sigma_{xx_i}\mathrm{d}A_i=E_{xx}I_i v_{i,xx}=D_{xx_i}v_{i,xx}$$

$$V_i=(E_{xx}I_i v_{i,xx})_{,x}+P_i v_{i,x}=-(D_{xx_i}v_{i,xx})_{,x}+P_i v_{i,x} \tag{4}$$

$$P_{i,x}=0 \qquad (D_{xx_i}v_{i,xx})_{,xx}-P_i v_{i,xx}=0 \tag{5}$$

where E_{xx} is the x-direction Young's modulus, A_i the region i cross-sectional area ($A_i=h_i$, $h_1=t$, $h_2=H$, $h_3=h$, and $h_4=t$), I_i the region i second moment of the cross-sectional area about the lateral in-plane axis z ($I_i=h_i^3/12$), and V_i the transverse shear load, needed for equilibrium.

§This is the case when the sides are free (wide column; $\sigma_{xx}=0$); in the case of a plate strip ($\epsilon_{zz}=0$), E_{xx} must be replaced by $E_{xx}/(1-\nu_{xz}\nu_{zx})$.

The boundary conditions, both in-plane and transverse, and the continuity conditions (kinematic and in internal loads) are as follows.

In-plane boundary conditions:

$$\text{at } x=0:\ u_1=0; \quad \text{at } x=L:\ P_4=-\bar{P} \tag{6}$$

Transverse boundary conditions:

1) Simple supports

$$\text{at } x=0:\ v_1=0 \text{ and } v_{1,xx}=0$$

$$\text{at } x=L:\ v_4=0 \text{ and } v_{4,xx}=0 \tag{7a}$$

2) Clamped supports

$$\text{at } x=0:\ v_1=0 \text{ and } v_{1,x}=0$$

$$\text{at } x=L:\ v_4=0 \text{ and } v_{4,x}=0 \tag{7b}$$

Kinematic continuity conditions:

at $x=\ell_1$

$$u_1-(H/2)v_{1,x}=u_3; \quad u_1+(h/2)v_{1,x}=u_2$$

$$v_1=v_2=v_3; \quad v_{1,x}=v_{2,x}=v_{3,x} \tag{8a}$$

at $x_1=\ell+a$

$$u_4-(H/2)v_{4,x}=u_3; \quad u_4+(h/2)v_{4,x}=u_2$$

$$v_2=v_3=v_4; \quad v_{2,x}=v_{3,x}=v_{4,x} \tag{8b}$$

Continuity in moments and forces:

at $x=\ell_1$

$$M_1-M_2-M_3+(H/2)P_3-(h/2)P_2=0$$

$$-V_1+V_2+V_3=0; \quad P_1-P_2-P_3=0 \tag{9a}$$

at $x=\ell_1+a$

$$M_2+M_3-M_4-(H/2)P_3+(h/2)P_2=0$$

$$-V_2-V_3+V_4=0; \quad P_2+P_3-P_4=0 \tag{9b}$$

where M_i, V_i, and P_i can be expressed in terms of the displacement gradients, through Eqs. (4) and (2).

A. Primary (Membrane) State Solution

As the compressive load P is applied (quasi) statically, the plate remains flat and a primary state solution is characterized by

$$v_i^P=0 \text{ and } u_i^P=\bar{A}_i x+\bar{B}_i \tag{10}$$

where $\bar{A}_i$ and $\bar{B}_i$ are arbitrary constants.

Use of the boundary and continuity conditions leads to complete knowledge of the primary state, or

$$v_i^P=0; \quad u_i^P=(P_i^P/C_{xx_i})x; \quad i=1,2,3,4 \tag{11}$$

and

$$P_1^P=P_4^P=-\bar{P}; \quad P_2^P=-(H/t)\bar{P}; \quad P_3^P=-(h/t)\bar{P} \tag{12}$$

$$M_i^P=0; \quad V_i^P=0; \quad i=1,2,3,4 \tag{13}$$

B. Buckling Equations

The buckling equations are derived by employing a perturbation method (Refs. 8-10), based on the concept of the existence of an adjacent equilibrium position at a bifurcation point (or at a limit point). The required steps are as follows: start with the equilibrium equations and proper boundary and interior continuity conditions, Eqs. (5-9), perturb them (from the primary state) by allowing small kinematically admissible changes in the displacement functions, make use of equilibrium at a point at which an adjacent equilibrium path is possible (critical point), and retain first-order terms in the admissible variations. The resulting linear ordinary-differential equations are the buckling equations. The corresponding boundary and continuity conditions are also obtained by perturbation technique.

The following expressions are substituted in Eqs. (5-9):

$$P_i = P_i^P + P_i^a; \quad u_i = u_i^P + u_i^a; \quad v_i = v_i^a$$

$$M_i = M_i^a; \quad V_i = V_i^a \tag{14}$$

where the superscript a parameters denote the small additional changes (that correspond to the admissible variations v_i^a and u_i^a). The buckling equations are

$$P_{i,x}^a = 0 \tag{15}$$

$$D_{xx_i} v_{i,xxx}^a - P_i^P v_{i,xx}^a = 0 \tag{16}$$

The related conditions are as follows.

In-plane boundary conditions:

$$\text{at } x=0: \quad u_1^a = 0; \quad \text{at } x=L: \quad P_4^a = 0 \tag{17}$$

Transverse boundary conditions:

1) Simple supports

$$\text{at } x=0: \quad v_1^a = 0 \text{ and } v_{1,xx}^a = 0$$

$$\text{at } x=L: \quad v_4^a = 0 \text{ and } v_{4,xx}^a = 0 \tag{18a}$$

2) Clamped supports

$$\text{at } x=0: \quad v_1^a = 0 \text{ and } v_{1,x}^a = 0$$

$$\text{at } x=L: \quad v_4^a = 0 \text{ and } v_{4,x}^a = 0 \tag{18b}$$

Kinematic continuity conditions:

at $x=\ell_1$

$$u_1^a - (H/2)v_{1,x}^a = u_3^a; \quad u_1^a + (h/2)v_{1,x}^a = u_2^a$$

$$v_1^a = v_2^a = v_3^a; \quad v_{1,x}^a = v_{2,x}^a = v_{3,x}^a \tag{19a}$$

at $x=\ell_1 + a$

$$u_3^a = u_4^a - (H/2)v_{4,x}^a; \quad u_2^a = u_4^a + (h/2)v_{4,x}^a$$

$$v_4^a = v_2^a = v_3^a; \quad v_{4,x}^a = v_{2,x}^a = v_{3,x}^a \tag{19b}$$

Continuity in moments and forces:

at $x=\ell_1$

$$M_1^a - M_2^a - M_3^a + P_3^a(H/2) - P_2^a(h/2) = 0$$

$$-V_1^a + V_2^a + V_3^a = 0; \quad P_1^a - P_2^a - P_3^a = 0 \tag{20a}$$

at $x=\ell_1 + a$

$$M_2^a + M_3^a - M_4^a - P_3^a(H/2) + P_2^a(h/2) = 0$$

$$-V_2^a - V_3^a + V_4^a = 0; \quad P_2^a + P_3^a - P_4^a = 0 \tag{20b}$$

C. Solution of Buckling Equations

The solution to the buckling equations can be written as

$$u_i^a = \bar{C}_{i1}x + \bar{C}_{i2} \tag{21a}$$

and

$$v_i^a = a_{i1}\sin k_i x + a_{i2}\cos k_{ix} + a_{i3}x + a_{i4} \tag{21b}$$

where $k_i^2 = -(P_i^P/D_{xx_i})$ and P_i^P are given by Eqs. (12) ($i=1,2,3,4$).

Note that, since the admissible variations in the displacement components can be made as small as one wishes, the reference surface strain can be linearized, or [see Eq. (2)]

$$(\epsilon_{xx_i}^0)^a = u_{i,x}^a \tag{22}$$

Thus, the expressions for the internal forces and moments become [see Eqs. (4)]

$$P_i^a = C_{xx_i} u_{i,x}^a; \quad M_i^a = D_{xx_i} v_{i,xx}^a; \quad V_i^a = -D_{xx_i} v_{i,xxx}^a + P_i^P v_{i,x}^a \tag{23}$$

Moreover, the solution to the buckling equations, Eqs. (21), requires knowledge of 24 constants ($\bar{C}_{i1}$, $\bar{C}_{i2}$, a_{ij}, $i=1,2,3,4$, and $j=1,2,3,4$,). There exist 24 boundary and continuity conditions, which are homogeneous in u_i^a, v_i^a and their space derivatives. These consist of two in-plane boundary conditions, Eqs. (17), four transverse boundary conditions, either Eqs. (18a) or Eqs. (18b), twelve kinematic continuity conditions, Eqs. (19a) and (19b), and six continuity conditions in moments and forces, Eqs. (20a) and (20b).

Use of the boundary conditions yields a system of linear, homogeneous algebraic equations in $\bar{C}_{i1}$, $\bar{C}_{i2}$, and a_{ij}. For a nontrivial solution to exist the determinant of the coefficients must vanish. The determinant contains geometric parameters and the applied load $\bar{P}$, because of the presence of P_i^P [see Eqs. (12)].

Before proceeding with the description and actual solution of the determinant, certain nondimensionalized parameters are introduced. These are

$$\bar{a} = \frac{a}{L}; \quad \bar{h} = \frac{h}{t}; \quad \bar{H} = \frac{H}{t} = 1 - \bar{h}$$

$$\bar{\lambda}^2 = \bar{P}L^2/D_{xx_1}; \quad \bar{p} = \bar{P}/P_{\text{cr}_{\text{perf}}}$$

$$\bar{p}_3 = \bar{P}_3/P_{\text{thin}}; \quad P_{\text{thin}} = 4\pi^2 D_{xx_3}/a^2 \tag{24}$$

$$P_{\text{cr}_{\text{perf}}} = \pi^2 D_{xx_1}/L^2 \text{ for simple supports}$$

$$= 4\pi^2 D_{xx_1}/L^2 \text{ for clamped supports}$$

Moreover, all a_{ij} coefficients [see Eqs. (21b)] have been changed to (v_i^a is dimensional; when divided by t it becomes nondimensionalized)

$$\bar{a}_{ij} = a_{ij}/t \qquad i=1,2,3,4; \quad j=1,2,4 \tag{25a}$$

and

$$\bar{a}_{i3} = a_{i3}L/t \text{ for all } i \tag{25b}$$

Depending on the boundary conditions [simple support (SS) or clamped] some of the constants are zero and others can easily be eliminated or expressed in terms of the remaining ones. For both sets of boundary conditions, the system of linear homogeneous algebraic equations is reduced in number to nine. These can be written in matrix form as

$$[F]\{X\} = 0 \tag{26}$$

where $[F]$ is a 9×9 matrix and $\{X\}$ a 1×9 (column) matrix.

The elements of the two matrices differ, depending on the boundary conditions. They are

$$\{X\}^T = (\bar{a}_{11}, \bar{a}_{13}, \bar{a}_{21}, \bar{a}_{22}, \bar{a}_{23}, \bar{a}_{31}, \bar{a}_{32}, \bar{a}_{41}, \bar{C}_{31}); \quad \text{SS}$$

$$= (\bar{a}_{11}, \bar{a}_{12}, \bar{a}_{21}, \bar{a}_{22}, \bar{a}_{23}, \bar{a}_{31}, \bar{a}_{32}, \bar{a}_{41}, \bar{C}_{31}); \quad \text{clamped} \qquad (27)$$

The elements of the $[F]$ matrix F_{ij} are listed in the Appendix.

As already mentioned, the characteristic equation is given by

$$|F_{ij}| = 0 \qquad (28)$$

and the lowest eigenvalue ($\bar{\lambda}$) is a measure of the critical load. Note that the elements of the determinant in Eq. (28) contain the geometric parameters, $\bar{h}$, $\bar{\ell}_1$, and $\bar{a}$ in addition to the load parameter $\bar{\lambda}$.

A computer program has been written for finding the critical load, $\bar{\lambda}_{cr}$, for various combinations of the geometric parameters.

III. Results

The Georgia Institute of Technology high-speed digital computer CDC-Cyber 70, Model 74-28, was employed for generating results. These results are presented both in tabular and graphical form.

Table 1 shows values of critical loads $\bar{p}$ of a clamped configuration with a symmetric delamination [see Eq. (24)], for several values of the delamination length parameter $\bar{a}$, and of the delamination thickness parameter $\bar{h}$. The last row gives the sum of the buckling loads of the two parts, if the delamination extends through the entire length $\bar{a}=1$. The sum $\bar{p}$ is a measure of the load carrying capacity of the completely damaged configuration

$$\bar{P}_{dam} = \frac{h^3}{(t)} + \frac{H^3}{(t)} = \bar{h}^3 + (1-\bar{h})^3 \qquad (29)$$

These results are also shown graphically in Fig. 2. It is clearly seen from these results that as long as $\bar{a} \leq \bar{h}$, the buckling load is not affected appreciably by the presence of the delamination, provided that the delamination thickness is relatively small ($\bar{h} \leq 0.2$). For the same condition of $\bar{a} \leq \bar{h}$, the presence of the delamination becomes more pronounced as one approaches a midthickness delamination ($\bar{h}=0.5$). Note that for this extreme case, when $\bar{a}=\bar{h}=0.5$, $\bar{P}_{cr}=0.69$ and $\bar{P}_{cr}$ increases as $\bar{a}$ becomes smaller and smaller. On the other hand, when $\bar{a} \geq \bar{h}$ the buckling load is greatly affected and it drops drastically, especially for the smaller values of the delamination thickness.

A comparison of the buckling loads with the buckling load for the completely damaged system (last number in each column) reveals certain observations which suggest related conclusions. When $\bar{a} \leq \bar{h}$ the values for $\bar{P}_{cr}$ are higher than $\bar{P}_{dam}$. This suggests that for these geometries the load carrying capacity of the system is related to and measured by the buckling load of the delaminated configuration. On the other hand, for $\bar{a} > \bar{h}$ buckling occurs at low values of the applied load. Then, if the load is further increased, this may lead to delamination growth and the damaged area may extend along the entire length of the system. This, of course, depends on the fracture toughness of the material, but the implication is that $\bar{P}_{dam}$ is a good lower bound for the load carrying capacity of the delaminated configuration. The problem of postbuckling behavior, delamination growth, and accurate estimation of the load carrying capacity of a delaminated configuration is the subject of another paper[11] by the same authors.

In Table 2, the value of the load in region 3 at the instant of buckling is given for the same range of parameters, $\bar{a}$ and $\bar{h}$, as in Table 1. These results are also for the case of clamped supports. The values for this region 3 load are nondimensionalized with respect to the critical load of the region 3 geometry, as if its ends were clamped. This is done primarily for finding the range of parameters $\bar{a}$ and $\bar{h}$ for which thin-film analysis holds.[3] Clearly, when $\bar{p}_3$ is close to

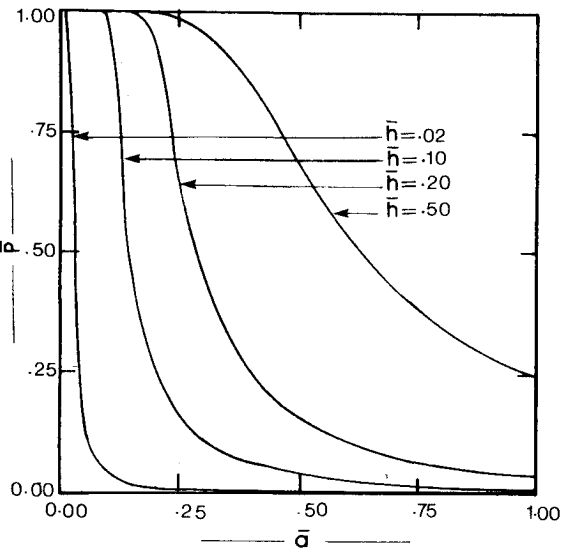

Fig. 2 Effect of symmetric delamination on buckling loads of wide column with clamped ends.

Table 1 Buckling loads for a symmetric delamination—clamped boundaries

$\bar{a}$ \ $\bar{h}$	0.02	0.05	0.1	0.2	0.3	0.4	0.5
0.025	0.6400	1.0000$^-$[a]	1.0000$^-$	1.0000$^-$	1.0000$^-$	1.0000$^-$	1.0000$^-$
0.05	0.1600	0.9949	1.0000$^-$	1.0000$^-$	1.0000$^-$	1.0000$^-$	1.0000$^-$
0.10	0.0400	0.2499	0.9799	0.9997	0.9998	0.9999	0.9999
0.15	0.0178	0.1111	0.4434	0.9966	0.9985	0.9989	0.9990
0.20	0.0100	0.0625	0.2495	0.9264	0.9924	0.9950	0.9956
0.25	0.0064	0.0400	0.1597	0.6256	0.9662	0.9835	0.9859
0.30	0.0044	0.0278	0.1109	0.6317	0.8582	0.9543	0.9638
0.40	0.0025	0.0152	0.0624	0.2470	0.5314	0.7883	0.8481
0.50	0.0016	0.0100	0.0400	0.1585	0.3469	0.5675	0.6896
0.60	0.0011	0.0069	0.0278	0.1103	0.2435	0.4124	0.5411
0.70	0.0008	0.0051	0.0204	0.0812	0.1804	0.3111	0.4310
0.80	0.0006	0.0039	0.0156	0.0623	0.1390	0.2428	0.3514
0.90	0.0005	0.0031	0.0123	0.0493	0.1105	0.1949	0.2923
1.00	0.0004	0.0025	0.0100	0.0400	0.0900	0.1600	0.2500
$\bar{P}_{dam}$	0.9412	0.8572	0.7300	0.5200	0.3700	0.2800	0.2500

[a] 1.000$^-$ indicates slightly smaller than one.

unity, thin-film analysis is applicable and, thus, delamination growth can be treated by the simpler analysis[3] developed for the case of thin-film behavior. Thin-film behavior implies that region 3 only experiences buckling and postbuckling deformations while the remainder of the plate remains undeformed. For small values of $\bar{h}$, say, $\bar{h} \leq 0.02$, thin-film is applicable for all values of $\bar{a}$. As $\bar{h}$ increases, toward its maximum value of 0.5, the region of applicability of thin-film analysis is confined toward the high $\bar{a}$-value region.

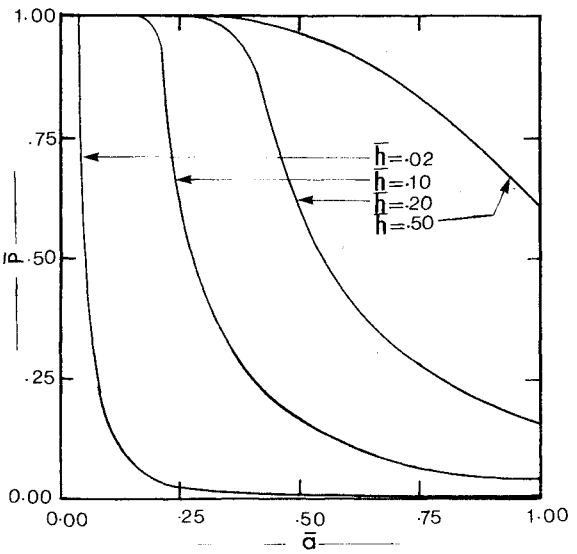

Fig. 3 Effect of symmetric delamination on buckling loads of wide column with simply supported ends.

Similar results are presented in Tables 3 and 4 and Fig. 3, respectively, for the case of simply supported ends. In Table 3, $\bar{p}$ is nondimensionalized with respect to the perfect geometry critical load for simply supported ends. The values corresponding to $\bar{p}_{\text{dam}}$ (last row) are the sum of the contributions of both parts acting independently of each other and both being simply supported. This may be questionable, because a better description of the completely damaged plate is needed. For example, if, when the delamination extends along the entire length, the thin part is lost (it becomes disconnected), then a better measure for P_{dam} would be $(1-h)^3$ rather than $\bar{h}^3+(1-\bar{h})^3$. It is also worth mentioning here that the values (P) corresponding to $\bar{a}=1$ (next to the last row) are calculated under the assumption that both parts (regions 3 and 2) have the same slope at the boundaries.

The trends, observed in the case of clamped supports, are also observed here but the regions seem to have shifted. For instance, in Table 1 it was observed that, as long as $\bar{a} \leq \bar{h}$, the buckling load was not affected appreciably by the presence of the delamination, for relatively small delamination thickness. In Table 3 this statement is also true, but $\bar{a} \leq \bar{h}$ must be replaced by $\bar{a} \leq 2\bar{h}$, and so on.

So far results have been presented and discussed for the case of symmetrically located delaminations $[\bar{\ell}_1 = 0.5(1-\bar{a})]$. Next, results are presented in Tables 5-8 for the case for which the delamination is asymmetrically located.

Tables 5 and 6 present results for the case of clamped supports, in terms of buckling loads $\bar{p}$ for various values of $\bar{h}$, and $\bar{\ell}_1$. The results in Table 5 correspond to $\bar{a}=0.1$ and those in Table 6 to $\bar{a}=0.2$. It is seen from Tables 5 and 6 that as

Table 2 Region of applicability of thin film analysis for a symmetric delaminated wide column with clamped ends

$\bar{a}$ \ $\bar{h}$	0.02	0.05	0.10	0.20	0.30	0.40	0.50
0.025	1.0000⁻	0.2500	0.0625	0.0156	0.0069	0.0039	0.0025
0.05	1.0000⁻	0.9949	0.2500	0.0625	0.0278	0.0156	0.0100
0.10	1.0000⁻	0.9998	0.9799	0.2499	0.1111	0.0625	0.0400
0.15	1.0000⁻	0.9998	0.9979	0.5606	0.4963	0.1405	0.0899
0.20	1.0000⁻	0.9998	0.9981	0.9264	0.4411	0.2488	0.1593
0.25	1.0000⁻	0.9998	0.9983	0.9775	0.6710	0.3842	0.2465
0.30	1.0000⁻	0.9998	0.9985	0.9835	0.8582	0.5368	0.3470
0.40	1.0000⁻	0.9998	0.9987	0.9882	0.9447	0.7883	0.5428
0.50	1.0000⁻	0.9999	0.9990	0.9909	0.9636	0.8868	0.6896
0.60	1.0000⁻	0.9999	0.9992	0.9931	0.9741	0.9279	0.7792
0.70	1.0000⁻	0.9999	0.9994	0.9950	0.9819	0.9528	0.8447
0.80	1.0000⁻	1.0000⁻	0.9996	0.9967	0.9885	0.9712	0.8996
0.90	1.0000⁻	1.0000⁻	0.9998	0.9984	0.9945	0.9865	0.9503
1.00	1.0000⁻	1.0000⁻	1.0000⁻	1.0000⁻	1.0000⁻	1.0000⁻	1.0000⁻

Table 3 Buckling loads for a symmetric delamination—simply supported boundaries

$\bar{a}$ \ $\bar{h}$	0.02	0.05	0.10	0.20	0.30	0.40	0.50
0.025	1.0000⁻	1.0000⁻	1.0000⁻	1.0000⁻	1.0000⁻	1.0000⁻	1.0000⁻
0.05	0.6400	1.0000⁻	1.0000⁻	1.0000⁻	1.0000⁻	1.0000⁻	1.0000⁻
0.10	0.1600	0.9929	1.0000⁻	1.0000⁻	1.0000⁻	1.0000⁻	1.0000⁻
0.15	0.0711	0.4431	0.9996	0.9999	0.9999	0.9999	0.9999
0.20	0.0400	0.2499	0.9723	0.9996	0.9997	0.9997	0.9997
0.25	0.0256	0.1600	0.6376	0.9979	0.9989	0.9991	0.9992
0.30	0.0178	0.1111	0.4432	0.7932	0.9971	0.9977	0.9980
0.40	0.0100	0.0625	0.2494	0.9016	0.9827	0.9902	0.9912
0.50	0.0064	0.0400	0.1596	0.6178	0.9402	0.9686	0.9729
0.60	0.0044	0.0278	0.1109	0.4331	0.8149	0.9198	0.9343
0.70	0.0033	0.0204	0.0815	0.3193	0.6484	0.8351	0.8703
0.80	0.0025	0.0156	0.0624	0.2450	0.5118	0.7264	0.7867
0.90	0.0020	0.0123	0.0493	0.1938	0.4106	0.6177	0.6966
1.00	0.0016	0.0100	0.0399	0.0399	0.3356	0.5229	0.6110
$\bar{P}_{\text{dam}}$	0.9412	0.8572	0.7300	0.5200	0.3700	0.2800	0.2500

Table 4 Region of applicability of thin film analysis for a symmetric delaminated wide column with simply supported ends

$\bar{a}$ \ $\bar{h}$	0.02	0.05	0.10	0.20	0.30	0.40	0.50
0.025	0.3906	0.0625	0.156	0.039	0.0017	0.0010	0.0006
0.05	1.0000$^-$	0.2500	0.0625	0.0156	0.0069	0.0039	0.0025
0.10	1.0000$^-$	0.9929	0.2500	0.0625	0.0278	0.0156	0.0010
0.15	1.0000$^-$	0.9997	0.5622	0.1406	0.0630	0.0352	0.0225
0.20	1.0000$^-$	0.9997	0.9723	0.2499	0.1111	0.0625	0.0400
0.25	1.0000$^-$	0.9997	0.9963	0.3898	0.1734	0.0976	0.0624
0.30	1.0000$^-$	0.9997	0.9971	0.5587	0.2493	0.1403	0.0898
0.40	1.0000$^-$	0.9997	0.9975	0.9016	0.4378	0.2476	0.1586
0.50	1.0000$^-$	0.9997	0.9977	0.9652	0.5454	0.3784	0.2432
0.60	1.0000$^-$	0.9997	0.9978	0.9744	0.6529	0.5174	0.3364
0.70	1.0000$^-$	0.9997	0.9978	0.9780	0.8826	0.6394	0.4265
0.80	1.0000$^-$	0.9997	0.9979	0.9800	0.9099	0.7264	0.5035
0.90	1.0000$^-$	0.9997	0.9979	0.9813	0.9238	0.7817	0.5643
1.00	1.0000$^-$	0.9997	0.9979	0.9822	0.9323	0.8170	0.6110

Table 5 Effect of delamination location on the buckling load (clamped supports; $\bar{a} = 0.1$)

$\bar{h}$ \ $\bar{\ell}_1$	0.0	0.1	0.2	0.3	0.45
0.50	0.249954	0.249951	0.249946	0.249942	0.249939
0.10	0.980866	0.987098	0.997582	0.986807	0.979920
0.20	0.999148	0.995863	0.993894	0.995898	0.999714
0.30	0.998706	0.992255	0.988500	0.992384	0.999825
0.40	0.998081	0.987930	0.982222	0.988242	0.999860
0.50	0.997744	0.985681	0.979017	0.986116	0.999868

Table 6 Effect of delamination location on the buckling load (clamped supports; $\bar{a} = 0.2$)

$\bar{h}$ \ $\bar{\ell}_1$	0.0	0.1	0.2	0.3	0.4
0.05	0.062493	0.062491	0.062489	0.062488	0.062487
0.10	0.249749	0.249689	0.249616	0.249557	0.249534
0.20	0.932757	0.947982	0.945508	0.930942	0.926444
0.30	0.955741	0.914213	0.919476	0.961344	0.992392
0.40	0.924773	0.865234	0.876756	0.940164	0.995044
0.50	0.905107	0.840507	0.855468	0.927749	0.995538

Table 7 Effect of delamination location on the buckling load (simple supports; $\bar{a} = 0.1$)

$\bar{h}$ \ $\bar{\ell}_1$	0.0	0.1	0.2	0.3	0.45
0.05	0.998639	0.996576	0.994855	0.993624	0.992901
0.10	0.999407	0.999511	0.999679	0.999847	0.999965
0.20	0.998517	0.998790	0.999232	0.999674	0.999985
0.30	0.997760	0.997760	0.998583	0.999409	0.999990
0.40	0.995823	0.996598	0.997849	0.999106	0.999991
0.50	0.995113	0.996020	0.997483	0.998954	0.999992

Table 8 Effect of delamination location on the buckling load (simple supports; $\bar{a} = 0.2$)

$\bar{h}$ \ $\bar{\ell}_1$	0.0	0.1	0.2	0.3	0.4
0.05	0.249936	0.269933	0.269931	0.249929	0.249929
0.10	0.988205	0.981420	0.976383	0.973308	0.972277
0.20	0.989043	0.991885	0.995416	0.998312	0.999429
0.30	0.979666	0.985074	0.991836	0.997459	0.999651
0.40	0.969003	0.977209	0.987545	0.996274	0.999719
0.50	0.963667	0.973241	0.985342	0.995645	0.999737

long as $\bar{h} \le \bar{a}$, the buckling load is the smallest, when the delamination is located symmetrically with respect to the midpoint of the wide column. On the other hand, when $\bar{h} > \bar{a}$ the buckling load is the smallest when the delamination is located in such a way that it spans the quarter point of the wide column.

For the case of simply supported columns the results of Tables 7 and 9 reveal similar trends. For $\bar{h} < \bar{a}$, the buckling load is the smallest when the delamination is located symmetrically with respect to the midpoint of the wide column. Finally, for $\bar{h} \ge \bar{a}$, the buckling load is the smallest when the delamination starts from the end of the wide column.

Note that in some cases, for $\bar{h} > \bar{a} = 0.2$ and clamped boundary conditions, the effect of delamination location on the buckling load is considerable. From Table 6 one observes that for $\bar{h} = 0.5$ $\bar{p}_{\min} = 0.841$ $(\bar{\ell}_1 = 0.1)$ while $\bar{p}_{\max} = 0.996$ $(\bar{\ell}_1 = 0.4)$.

IV. Conclusions

A simple model has been employed to study delamination buckling and the effect of location, size, and thickness of delamination on the buckling load. The simplicity of the model limits the applicability of the results to the case for which each layer is made out of the same, either orthotropic or isotropic materials. For the case of laminates the present results are not applicable, because there exists coupling between bending and extension and therefore there is no buckling (in the classical sense of bifurcation from a primary momentless state). For these geometries (laminates) the results serve a different purpose. They can be employed to relate the ultimate load carrying capacity of the completely (throughout) damaged laminate to the allowable for the delaminated laminate.

A good application of the present analysis and results is in the analysis of adhesive bonding of two similar materials.[12]

Appendix A

The elements of the $[F]$ matrix, F_{ij} [see Eq. (26)], are listed below. The top expression corresponds to the case of simple supports and the bottom to that of clamped supports. If there is only one expression, it is applicable to both.

$$F_{11} = 0; \quad F_{12} = 0$$

$$F_{13} = \frac{\bar{h}}{1-\bar{h}}\left[\cos\frac{\bar{\lambda}(\bar{\ell}_1+\bar{a})}{1-\bar{h}} - \cos\frac{\bar{\lambda}\bar{\ell}_1}{\bar{h}}\right]$$

$$F_{14} = -\frac{\bar{h}}{1-\bar{h}}\left[\sin\frac{\bar{\lambda}(\bar{\ell}_1+\bar{a})}{1-\bar{h}} - \sin\frac{\bar{\lambda}\bar{\ell}_1}{1-\bar{h}}\right]; \quad F_{15} = 0$$

$$F_{16} = \frac{1-\bar{h}}{\bar{h}}\left[\cos\frac{\bar{\lambda}(\bar{\ell}_1+\bar{a})}{\bar{h}} - \cos\frac{\bar{\lambda}\bar{\ell}_1}{\bar{h}}\right]$$

$$F_{17} = -\frac{1-\bar{h}}{\bar{h}}\left[\sin\frac{\bar{\lambda}(\bar{\ell}_1+\bar{a})}{\bar{h}} - \sin\frac{\bar{\lambda}\bar{\ell}_1}{\bar{h}}\right]$$

$$F_{18} = = 0; \quad F_{19} = \frac{2\pi^2\bar{h}^2}{2\bar{\lambda}\bar{a}(1-\bar{h})}$$

$$F_{21} = \begin{cases} \sin\bar{\lambda}\bar{\ell}_1 \\ \sin\bar{\lambda}\bar{\ell}_1 + \sin\bar{\lambda}(1-\bar{\ell}_1-\bar{a}) - \bar{\lambda}(1-\bar{a}) \\ \quad -\cot\lambda\{1-\cos(1-\bar{\ell}_1-\bar{a})\} \end{cases}$$

$$F_{22} = \begin{cases} 1-\bar{a} \\ \cos\bar{\lambda}\bar{\ell}_1 - 1 \end{cases}$$

$$F_{23} = -\frac{1-\bar{h}}{\bar{h}}F_{14}; \quad F_{24} = \frac{1-\bar{h}}{\bar{h}}F_{13}; \quad F_{25} = \bar{a}; \quad F_{26} = 0; \quad F_{27} = 0$$

$$F_{28} = \begin{cases} -\sin\bar{\lambda}\bar{\ell} \\ 1-\cos\bar{\lambda}(1-\bar{\ell}_1-\bar{a}) \end{cases} \quad F_{29} = 0$$

$$F_{31} = \begin{cases} \sin\bar{\lambda}\bar{\ell}_1 \\ \sin\bar{\lambda}\bar{\ell}_1 + \sin\bar{\lambda}(1-\bar{\ell}_1-\bar{a}) - \bar{\lambda}\left(1+\bar{a}\dfrac{1-\bar{h}}{\bar{h}}\right) \\ \quad -\cot\bar{\lambda}[1-\cos\bar{\lambda}(1-\bar{\ell}_1-\bar{a})] \end{cases}$$

$$F_{32} = \begin{cases} 1+\bar{a}\dfrac{1-\bar{h}}{\bar{h}} \\ \\ \cos\bar{\lambda}\bar{\ell}_1 - 1 \end{cases}; \quad F_{33} = F_{34} = 0; \quad F_{35} = -\bar{a}\frac{1-\bar{h}}{\bar{h}}$$

$$F_{36} = \sin\frac{\bar{\lambda}(\bar{\ell}_1+\bar{a})}{\bar{h}} - \sin\frac{\bar{\lambda}\bar{\ell}_1}{\bar{h}}$$

$$F_{37} = \cos\frac{\bar{\lambda}(\bar{\ell}_1+\bar{a})}{\bar{h}} - \cos\frac{\lambda\ell_1}{\bar{h}}$$

$$F_{38} = \begin{cases} -\sin\bar{\lambda}(1-\bar{\ell}_1-\bar{a}) \\ 1-\cos\bar{\lambda}(1-\bar{\ell}_1-\bar{a}) \end{cases}; \quad F_{39} = 0$$

$$F_{41} = \begin{cases} \bar{\lambda}\cos\bar{\lambda}\bar{\ell}_1 \\ \bar{\lambda}\cos\bar{\lambda}\bar{\ell}_1 - \bar{\lambda} \end{cases}$$

$$F_{42} = \begin{cases} 1 \\ -\bar{\lambda}\sin\bar{\lambda}\bar{\ell}_1 \end{cases}; \quad F_{43} = -\frac{\bar{\lambda}}{1-\bar{h}}\cos\frac{\bar{\lambda}\bar{\ell}_1}{1-\bar{h}}$$

$$F_{44} = \frac{\bar{\lambda}}{1-\bar{h}}\sin\frac{\bar{\lambda}\bar{\ell}_1}{1-\bar{h}}; \quad F_{45} = -1; \quad F_{46} = F_{47} = F_{48} = F_{49} = 0$$

$$F_{51} = \begin{cases} \bar{\lambda}\cos\bar{\lambda}\bar{\ell}_1 \\ \bar{\lambda}\cos\bar{\lambda}\bar{\ell}_1 + \bar{\lambda}(1-\bar{h})/\bar{h} \end{cases}$$

$$F_{52} = \begin{cases} -(1-\bar{h})/\bar{h} \\ -\bar{\lambda}\sin\bar{\lambda}\bar{\ell}_1 \end{cases}; \quad F_{53} = F_{54} = 0$$

$$F_{55} = \frac{1-\bar{h}}{\bar{h}}; \quad F_{56} = -\frac{\bar{\lambda}}{\bar{h}}\cos\frac{\bar{\lambda}\bar{\ell}_1}{\bar{h}}$$

$$F_{57} = \frac{\bar{\lambda}}{\bar{h}}\sin\frac{\bar{\lambda}\bar{\ell}_1}{\bar{h}}; \quad F_{58} = F_{59} = 0$$

$$F_{61} = \begin{cases} 0 \\ \bar{\lambda}[\cos\bar{\lambda}(1-\bar{\ell}_1-\bar{a}) - 1] - \bar{\lambda}\cot\bar{\lambda}\sin\bar{\lambda}(1-\bar{\ell}_1-\bar{a}) \end{cases}$$

$$F_{62} = \begin{cases} 1 \\ 0 \end{cases}; \quad F_{63} = -\frac{\bar{\lambda}}{1-\bar{h}}\cos\frac{\bar{\lambda}(\bar{\ell}_1+\bar{a})}{1-\bar{h}}$$

$$F_{64} = \frac{\bar{\lambda}}{1-\bar{h}}\sin\frac{\bar{\lambda}(\bar{\ell}_1+\bar{a})}{1-\bar{h}}; \quad F_{65} = -1; \quad F_{66} = F_{67} = 0$$

$$F_{68} = \begin{cases} -\bar{\lambda}\cos\bar{\lambda}(1-\bar{\ell}_1-\bar{a}) \\ \bar{\lambda}\sin\bar{\lambda}(1-\bar{\ell}_1-\bar{a}) \end{cases}; \quad F_{69} = 0$$

$$F_{71} = \begin{cases} 0 \\ \bar{\lambda}\left[\cos\bar{\lambda}(1-\bar{\ell}_1-\bar{a}) + \dfrac{1-\bar{h}}{\bar{h}}\right] - \bar{\lambda}\cot\bar{\lambda}\sin\bar{\lambda}(1-\bar{\ell}_1-\bar{a}) \end{cases}$$

$$F_{72} = \begin{cases} (-1-\bar{h})/\bar{h} \\ 0 \end{cases}; \quad F_{73} = F_{74} = 0; \quad F_{75} = (1-\bar{h})/\bar{h}$$

$$F_{76} = \frac{\bar{\lambda}}{\bar{h}}\cos\frac{\bar{\lambda}(\bar{\ell}_1+\bar{a})}{\bar{h}}; \quad F_{77} = \frac{\bar{\lambda}}{\bar{h}}\sin\frac{\bar{\lambda}(\bar{\ell}_1+\bar{a})}{\bar{h}}$$

$$F_{78}=\begin{cases}-\bar{\lambda}\cos\bar{\lambda}(1-\bar{\ell}_1-\bar{a})\\ \bar{\lambda}\sin\bar{\lambda}(1-\bar{\ell}_1-\bar{a})\end{cases};\quad F_{79}=0$$

$$F_{81}=\sin\bar{\lambda}\bar{\ell}_1;\ F_{82}=\begin{cases}0\\ \cos\lambda\ell_1\end{cases}$$

$$F_{83}=-(1-\bar{h})\sin\frac{\bar{\lambda}\bar{\ell}_1}{\bar{h}};\ F_{84}=-(1-\bar{h})\cos\frac{\bar{\lambda}\bar{\ell}_1}{1-\bar{h}}$$

$$F_{85}=0;\quad F_{86}=-\bar{h}\sin\frac{\bar{\lambda}\bar{\ell}_1}{\bar{h}}$$

$$F_{87}=-\bar{h}\cos\frac{\bar{\lambda}\bar{\ell}_1}{\bar{h}};\ F_{88}=0;\quad F_{89}=\frac{2\pi^2\bar{h}^3}{\bar{\lambda}^2\bar{a}^2}$$

$$F_{91}=\begin{cases}0\\ -\sin\bar{\lambda}(1-\bar{\ell}_1-\bar{a})-\cot\bar{\lambda}\cos\bar{\lambda}(1-\bar{\ell}_1-\bar{a})\end{cases}$$

$$F_{93}=-(1-\bar{h})\sin\frac{\bar{\lambda}(\bar{\ell}_1+\bar{a})}{\bar{h}};\ F_{94}=(1-\bar{h})\cos\frac{\bar{\lambda}(\bar{\ell}_1+\bar{a})}{1-\bar{h}}$$

$$F_{95}=0;\ F_{96}=-\bar{h}\sin\frac{\bar{\lambda}(\bar{\ell}_1+\bar{a})}{\bar{h}};\ F_{97}=-\bar{h}\cos\frac{\bar{\lambda}(\bar{\ell}_1+\bar{a})}{\bar{h}}$$

$$F_{98}=\begin{cases}\sin\bar{\lambda}(1-\bar{\ell}_1-\bar{a})\\ \cos\bar{\lambda}(\bar{\ell}_1+\bar{a})\end{cases};\ F_{99}=F_{89}$$

Acknowledgments

The work is performed under the United States Air Force Office of Scientific Research, AFOSR Grant 83-0243. The authors gratefully acknowledge this financial support and express their thanks to the Program Manager, Dr. Anthony K. Amos, for his encouragement and many fruitful discussions.

References

[1]Wilkins, D. J., Eisermann, J. R., Camin, R. A., Margolis, W. S., and Benson, R. A., "Characterizing Delamination Growth in Graphite-Epoxy," *Damage in Composite Materials*, ASTM STP 775, edited by K. L. Reifsnider, 1982, pp. 168-183.

[2]Troshin, V. P., "Effect of Longitudinal Delamination in a Laminar Cylindrical Shell on the Critical External Pressure," *Journal of Composite Materials*, Vol. 17, No. 5, 1983, pp. 563-567 (translated from *Mekhanika Kompozitnykh Materialov*, No. 5, 1982, pp. 839-843).

[3]Chai, H., Babcock, C. D., and Knauss, W., "One Dimensional Modelling of Failure in Laminated Plates by Delamination Buckling," *Journal of Solids and Structures*, Vol. 17, No. 11, 1981, pp. 1069-1083.

[4]Whitcomb, J. D., "Finite Element Analysis of Instability-Related Delamination Growth," *Journal of Composite Materials*, Vol. 15, 1981, pp. 403-426.

[5]Yin, W. L., and Wang, J.T.S., "Postbuckling Growth of a One-Dimensional Delamination. Part I. Evaluation of the Energy Release Rate," *Journal of Applied Mechanics*, submitted for publication, 1983.

[6]Yin, W. L., "Axisymmetric Buckling and Growth of a Circular Delamination in a Compressed Laminate," *International Journal of Solids and Structures*, submitted for publication, 1983.

[7]Bottega, W. J. and Maewall, A., "Delamination Buckling and Growth in Laminates," *Journal of Applied Mechanics*, Vol. 50, No. 1, 1983, pp. 184-189.

[8]Bellman, R., *Perturbation Techniques in Mathematics, Physics and Engineering*, Holt, Rinehart and Winston, New York, 1969.

[9]Sewell, M. J., "The Static Perturbation Technique in Buckling Problems," *Journal of Mechanics and Physics of Solids*, Vol, 13, 1965, pp. 247-254.

[10]Simitses, G. J., *Elastic Stability of Structures*, Prentice-Hall Inc., Englewood Cliffs, N.J., 1976, Chap. 7.

[11]Yin, W.-L., Sallam, S., and Simitses, G. J., "Ultimate Axial Load Capacity of a Delaminated Plate," AIAA Paper 84-08-92, May 1984.

[12]Chow, C. L. and Ngan, K. M., "Method of Fracture Toughness Evaluation of Adhesive Joints," *Journal of Strain Analysis*, Vol. 15, No. 2, 1980, pp. 97-101.